Two-way Coupling of Fluids to Rigid and Deformable Solids and Shells

Avi Robinson-Mosher* Stanford University
Tamar Shinar* Stanford University
Jon Gretarsson* Stanford University
Jonathan Su* Stanford University, Intel
Ronald Fedkiw* Stanford University, Industrial Light + Magic

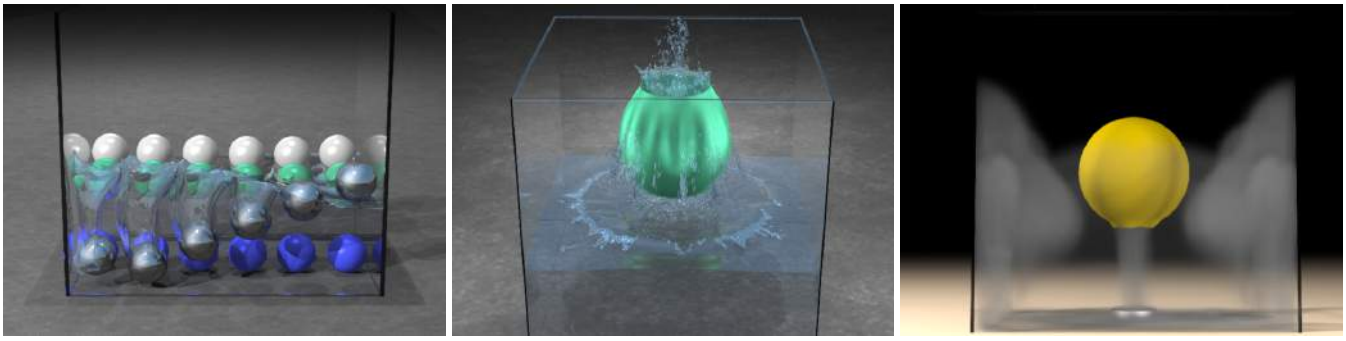

Figure 1: *(Left) Many rigid balls with varying densities plunge into a pool of water. (Center) Water splashes out of an elastic cloth bag. (Right) A balloon shoots upwards, releasing a jet of smoke.*

Abstract

We propose a novel solid/fluid coupling method that treats the coupled system in a fully implicit manner making it stable for arbitrary time steps, large density ratios, etc. In contrast to previous work in computer graphics, we derive our method using a simple back-of-the-envelope approach which lumps the solid and fluid momenta together, and which we show exactly conserves the momentum of the coupled system. Notably, our method uses the standard Cartesian fluid discretization and does not require (moving) conforming tetrahedral meshes or ALE frameworks. Furthermore, we use a standard Lagrangian framework for the solid, thus supporting arbitrary solid constitutive models, both implicit and explicit time integration, etc. The method is quite general, working for smoke, water, and multiphase fluids as well as both rigid and deformable solids, and both volumes and thin shells. Rigid shells and cloth are handled automatically without special treatment, and we support fully one-sided discretizations without leaking. Our equations are fully symmetric, allowing for the use of fast solvers, which is a natural result of properly conserving momentum. Finally, for simple explicit time integration of rigid bodies, we show that our equations reduce to a form similar to previous work via a single block Gaussian elimination operation, but that this approach scales poorly, i.e. as though in four spatial dimensions rather than three.

CR Categories: I.3.5 [Computer Graphics]: Computational Geometry and Object Modeling—Physically based modeling

Keywords: Two-way solid/fluid coupling, stability

*e-mail: {avir,shinar,jontg,jonsu,fedkiw}@cs.stanford.edu

1 Introduction

Simulation of the physical interaction at solid/fluid interfaces has been the subject of much recent work in computational physics as well as in computer graphics. Typically the effect of the solid on the fluid is modeled by taking the solid velocity as a boundary condition for the fluid solve. Conversely, the effect of the fluid on the solid is determined by integrating the fluid pressure along the solid boundary to compute a force on the solid. This basic approach has been employed both in an interleaved fashion, solving the solid or fluid system separately at each step using the results of the previous step, as well as in a fully coupled fashion where the fluid and solid equations are solved simultaneously in one combined system. In general, neither the interleaved nor the coupled treatments conserve momentum at the solid/fluid interface, and this lack of conservation negatively impacts both accuracy and stability of the overall simulation, especially in the case of stiff coupling problems or large time steps where large errors can lead to large velocities if momentum is not conserved.

In this paper, we instead derive our equations from the physical principle that momentum should be conserved at the solid/fluid boundary subject to the constraint that the relative velocities are zero. In addition to conserving momentum and enforcing the no-slip boundary condition, our approach utilizes the standard Cartesian Eulerian grid for the fluid and Lagrangian mesh for the solid and results in a sparse, symmetric linear system. The method is sufficiently general to treat rigid, deformable, volumetric and thin solids coupled to multiphase incompressible flow.

2 Related Work

State-of-the-art solvers typically use Eulerian methods for fluids and Lagrangian methods for solids, but it has proven difficult to couple these disparate simulation methods together. Thus, many researchers have taken a fully Lagrangian approach [Terzopoulos et al. 1989; Hadap and Magnenat-Thalmann 2001; Müller et al. 2004a; Müller et al. 2004b; Keiser et al. 2005; Yuksel et al. 2007; Bargteil et al. 2007], e.g. using particle-based methods for both the fluid and the solid ([Müller et al. 2004a; Keiser et al. 2005]). Alternatively, one could use Eulerian methods for both the fluid and the solid, treating solids as high viscosity or viscoelastic Eulerian fluids [Carlson et al. 2002; Rasmussen et al. 2004; Goktekin et al.

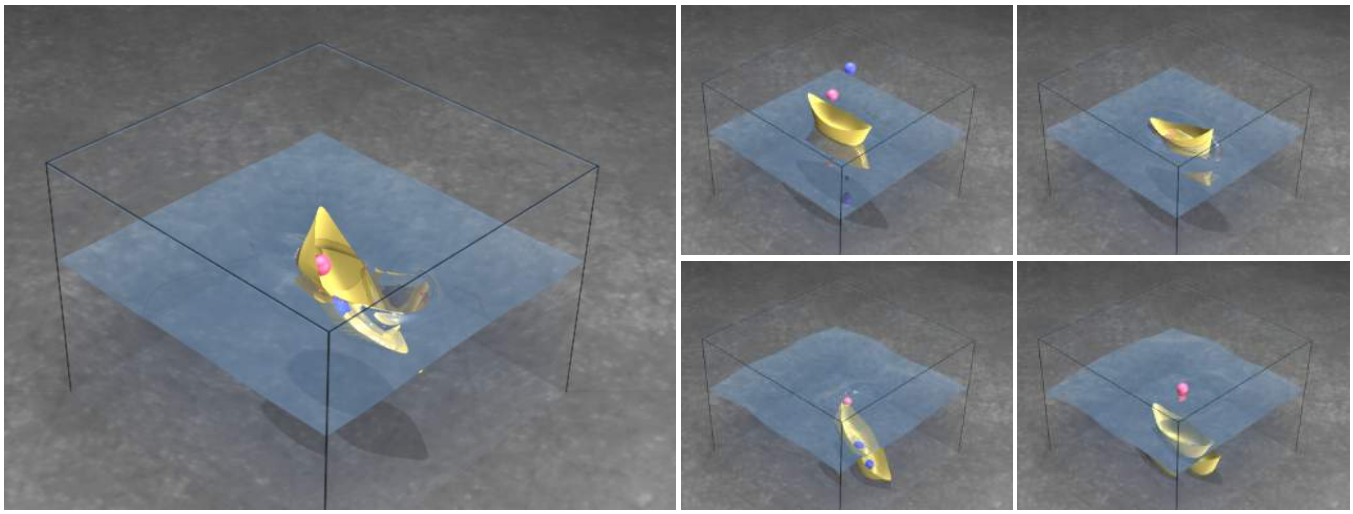

Figure 2: *A light sphere and then a heavy sphere are dropped into a thin shell rigid boat floating in a pool of water (160 × 120 × 160 fluid grid). The light sphere barely rocks the boat, while the heavy sphere sinks it, and the light sphere bobs back to the surface.*

2004; Losasso et al. 2006b]. See also [Faure et al. 2007] for an interesting approach that applies an Eulerian contact model based on implicitly integrated repulsion forces to various simulation objects including Smoothed Particle Hydrodynamics fluid with thin deformable shells and an Eulerian fluid with volumetric rigid and deformable solids.

Coupling an Eulerian fluid to a Lagrangian solid is typically accomplished using the solid velocity as a boundary condition for the fluid while integrating the pressure force on the surface of the solid, e.g. [Yngve et al. 2000; Génevaux et al. 2003; Carlson et al. 2004; Guendelman et al. 2005; Losasso et al. 2006a]. These approaches treat coupling in either an explicit or semi-implicit fashion and thus stability and accuracy issues remain. For example, [Carlson et al. 2004; Guendelman et al. 2005; Losasso et al. 2006a] solve a Poisson equation with the solid density rasterized onto the fluid grid alleviating some stability issues, but this rasterization does not account for the rigidity of objects, internal elastic forces, etc. Afterwards, [Carlson et al. 2004] projects the velocity field pertaining to the rigid body to enforce rigidity, but this creates a discontinuous velocity which allows fluid to leak into and out of the solid. [Guendelman et al. 2005; Losasso et al. 2006a] instead only use the Poisson equation to calculate forces on the solid, and afterwards project the fluid to be consistent with the resulting solid velocity in order to prevent leaking – however, this makes the method less stable.

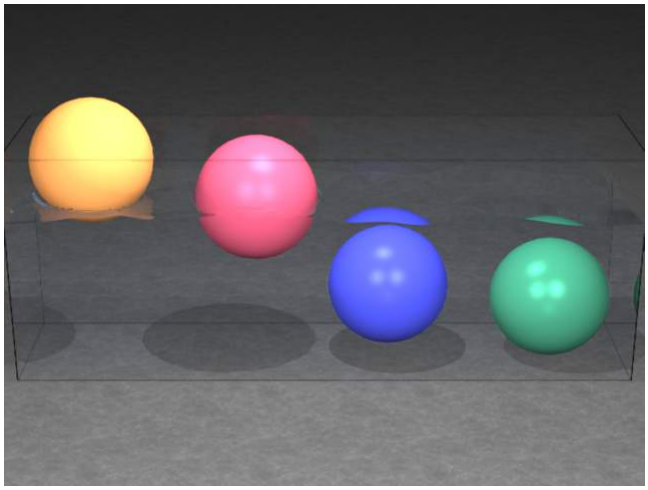

Figure 3: *We demonstrate that our method handles buoyancy correctly by releasing rigid spheres of varying density in a pool of water (200 × 75 × 50 fluid grid).*

[Klingner et al. 2006; Chentanez et al. 2006; Batty et al. 2007] consider fully implicit stable two-way coupled interactions between solids and fluids. [Klingner et al. 2006; Batty et al. 2007] are limited to rigid bodies, and although they add only a rank 6 update per body to their fluid Poisson matrix, the resulting number of elements scales like a four spatial dimensional problem instead of three. [Chentanez et al. 2006] addresses deformable objects, but obtains a non-symmetric discretization. These methods do not address rigid shells or cloth.

The straightforward method of using Neumann boundary conditions on the fluid and integrating the pressure force on the boundary of the solid as used in [Guendelman et al. 2005; Losasso et al. 2006a] and the Eulerian version of [Chentanez et al. 2006] does not conserve momentum. Thus even though [Chentanez et al. 2006] proposes a fully implicit coupling, the Eulerian version of their method can still be unstable and yield nonphysical behavior. The key to fixing this is to properly and conservatively account for all pressure forces that transmit momentum between fluid and solid, as our formulation does while yielding a symmetrically coupled system. Unlike their Cartesian counterparts, Arbitrary Lagrangian-Eulerian (ALE) meshes can more readily be made to conserve momentum as long as the solid/fluid boundary faces are treated in the same conservative fashion as internal fluid/fluid faces. However, ALE methods require moving meshes that can lead to poor aspect ratios requiring frequent remeshing, and thus we prefer an Eulerian approach. Moreover, it would be difficult to create an ALE fluid mesh that conforms to a deforming piece of cloth.

3 Motivation

Consider a two-dimensional example of an axis-aligned interface, and a particular dual cell (a staggered cell between two pressure samples in the standard MAC grid discretization) which is half filled with each of two distinct materials with densities ρ_1 and ρ_2

(Figure 4). This simple case degenerates into a one-dimensional problem. Given the constraint that the materials remain in contact, moving together, we can compute the pressure gradient's contribution to each material. If the pressure at the interface between the materials is $p_{i+1/2}$ at $x_{i+1/2}$, then conservation of momentum gives

$$\frac{Du_1}{Dt} = \frac{p_i - p_{i+1/2}}{\Delta x \rho_1/2} \text{ and } \frac{Du_2}{Dt} = \frac{p_{i+1/2} - p_{i+1}}{\Delta x \rho_2/2}. \quad (1)$$

The constraint that the interface remain in contact implies that $Du_1/Dt = Du_2/Dt$, and thus

$$p_{i+1/2} = (\rho_2 p_i + \rho_1 p_{i+1})/(\rho_1 + \rho_2). \quad (2)$$

When $\rho_1 = \rho_2$, the pressure profile is linear as illustrated by the red line in Figure 4. When ρ_1 is larger (smaller) than ρ_2, the pressure profile instead looks like the black (green) line.

We next consider the momentum update equation

$$\mathbf{u}^{n+1} = \mathbf{u}^\star - (\Delta t/\rho)\nabla p \quad (3)$$

used by [Batty et al. 2007] to derive their kinetic energy minimization. Scaling by the volume of fluid in the dual cell, V_F, we obtain

$$M_F \mathbf{u}^{n+1} = \rho V_F \mathbf{u}^{n+1} = \rho V_F \mathbf{u}^\star - V_F \Delta t \nabla p, \quad (4)$$

where M_F is the mass of the fluid in the dual cell. Thus the total pressure-based impulse transferred to the cell is given by $\Delta t V_{DC} \nabla p$ where V_{DC} is the total volume of the dual cell, and [Batty et al. 2007] transfer V_F/V_{DC} of this impulse to the fluid and $(V_{DC} - V_F)/V_{DC}$ to the solid. The amount of impulse transferred to each material depends only on the volume of that material in cell, equivalent to the red line in Figure 4. The impulse distribution necessary to maintain contact varies with the material densities, as shown above, so this gives a nonphysical result in most cases, exacerbated in the case of thin shells, which have zero volume. Note that while [Batty et al. 2007] computes a nonphysical pressure profile within a single dual cell, the ghost-like pressures interior to the volumetric rigid bodies in their method allow them to maintain velocity compatibility between the solid and the fluid. However, since the force is distributed incorrectly in space, this may result in an incorrect torque. The result of replacing the coupling component of our time integration (see Section 7) with that of [Batty et al. 2007] is shown in Figure 5.

Given that this kinetic energy formulation admits a nonphysical answer in our simple one-dimensional example, we prefer a back-of-the-envelope type approach as described above, where we lump the

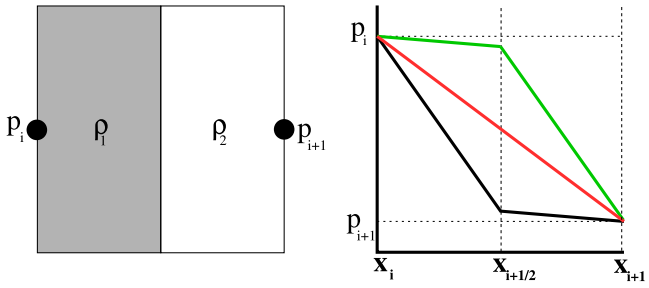

Figure 4: *(Left) A two-dimensional drawing of a dual cell containing two materials of different densities. (Right) A graph of the pressure profile on a cross-section through the cell connecting p_i to p_{i+1}, i.e. $\boldsymbol{x_i}$ to $\boldsymbol{x_{i+1}}$.*

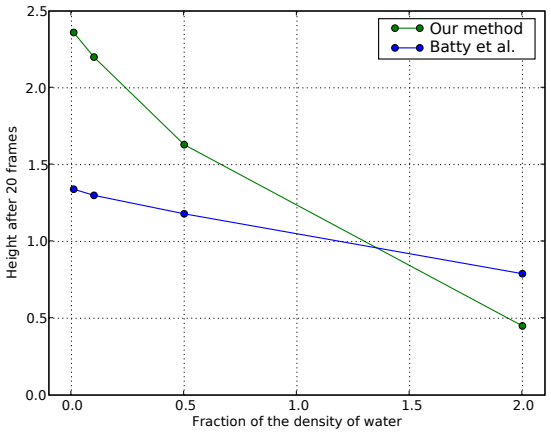

Figure 5: *A graphical comparison between our coupling method and that of Batty et al. illustrating the relationship between rise rate and density of fully immersed rigid spheres starting from rest at height 1.*

fluid and solid together assuming that they move at the same velocity, compute the change in momentum for the combined system, and then unlump the materials computing the respective pressure gradient for each. That is, our computational approach to treating mixed solid/fluid cells is to map the fluid mass and momentum to the solid nodes, calculate conservation of momentum as usual on each node of the solid taking into account the added fluid quantities, and finally remap the fluid velocities back to the Cartesian grid. We solve for cells which are completely filled with fluid as usual, meaning that the overall fluid discretization looks like that of a typical voxelized solid. The only difference is that the mixed dual cells are not treated as completely solid, but instead treated using our computational version of the back-of-the-envelope calculation. Similarly, the solid discretization proceeds in standard fashion, except that we lump some extra mass and momentum onto the solid nodes.

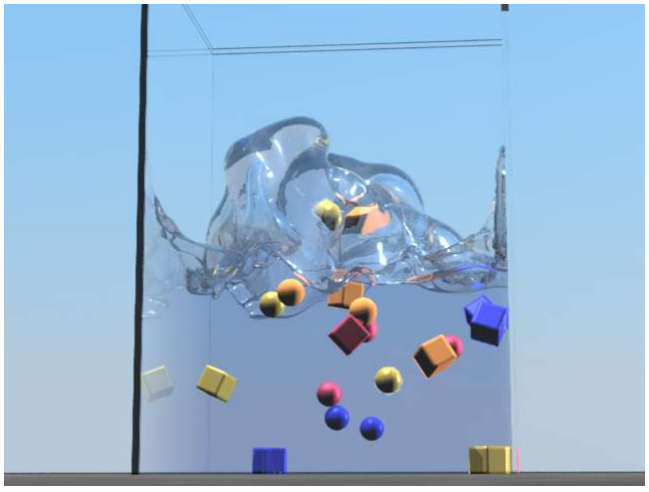

Figure 6: *Many rigid bodies circulate in a turbulent fountain, demonstrating scalability and dynamic interactions between rigid bodies (i.e. collisions) (100 × 150 × 100 fluid grid).*

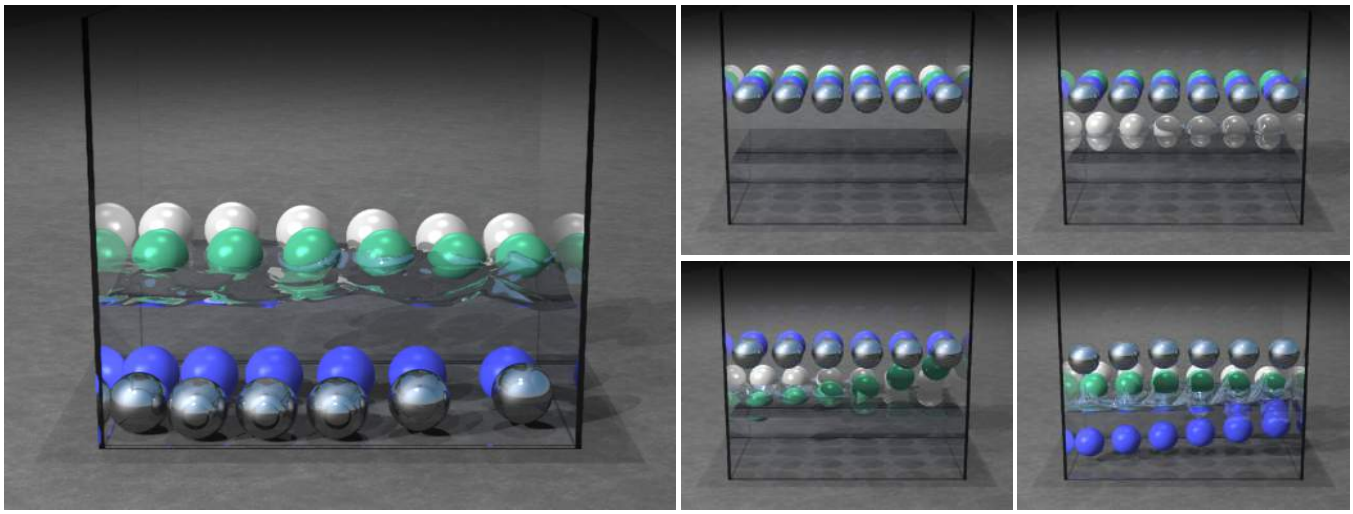

Figure 7: *24 rigid spheres of varying density are dropped into a pool of water, demonstrating scalability to many bodies (225 × 300 × 150 fluid grid).*

4 Conservation of Momentum

We discretize the fluid momentum equations in typical fashion, splitting them into the calculation of an intermediate velocity followed by a pressure projection to obtain a divergence free velocity field.

$$\frac{\mathbf{u}^\star - \mathbf{u}^n}{\Delta t} + \mathbf{u} \cdot \nabla \mathbf{u} = \mathbf{f} \tag{5}$$

$$\frac{\mathbf{u}^{n+1} - \mathbf{u}^\star}{\Delta t} + \frac{\nabla p}{\rho} = \mathbf{0} \tag{6}$$

For purposes of solid/fluid coupling it makes sense to consider Equation (6) in control volume form. In a standard MAC grid discretization the control volumes for the velocity appear on different dual cells surrounding the faces. For the u velocity the dual cells are the regular cells shifted to the left and right by $\Delta x/2$, for the v velocity they are shifted up and down by $\Delta y/2$, etc.

First consider the dual cells for the u velocity, where we have

$$Mu^{n+1} - Mu^\star + \Delta t V p_x = 0 \tag{7}$$

where $\rho = M/V$. This equation states that the net change of momentum in the cell is given by the pressure forces on the boundary, i.e.

$$\begin{aligned} Vp_x = &\quad (\Delta x \Delta y \Delta z)(p_{i+1} - p_i)/\Delta x \\ = &\quad \Delta y \Delta z p_{i+1} - \Delta y \Delta z p_i, \end{aligned} \tag{8}$$

indicating that the pressure contribution to this cell is simply obtained by multiplying the pressure on the left and right faces by the area of the cell face. Thus we can rewrite Equation (7) as

$$Mu^{n+1} - Mu^\star + \Delta t A(p_{i+1} - p_i) = 0. \tag{9}$$

Note that here M represents the mass of the whole dual cell, A the area of the whole face, and p_{i+1} and p_i are defined across the whole face. Thus for a mixed dual cell which has both solids and fluids in it, this equation represents the net change in momentum for the cell.

If one were solving only for the fluid component in the dual cell, M should only represent the mass of fluid, and one would have to decide what portion of the impulse $-\Delta t A(p_{i+1} - p_i)$ is allocated to the fluid and what portion is allocated to the solid, as in our example in Section 3. That is, the fluid update equation would look like

$$M_F u_F^{n+1} - M_F u_F^\star + \Delta t A(p_{i+1} - p_i) + I_{DC} = 0 \tag{10}$$

where I_{DC} is the momentum transferred to the solid.

Conservation of momentum on the solid nodes can be written as

$$M_S \mathbf{V}_S^{n+1} = M_S \mathbf{V}_S^\star + \Delta t D \mathbf{V}_S^{n+1} + W^T \mathbf{I} \tag{11}$$

where M_S is the mass of the solid, $\mathbf{V}_S$ is the solid velocity, $\mathbf{V}_S^\star$ includes all of the explicitly integrated forces, and D is the coefficient matrix for the implicitly integrated damping forces. $W^T \mathbf{I}$ represents the momentum transfer from fluid to solid, where $\mathbf{I}$ is a vector containing all the I_{DC} values from the dual cells which contain both fluid and solid, and W^T conservatively partitions this momentum among all of the solid nodes.

The time integration can be explicit, semi-implicit, or fully implicit. For fully explicit time integration of the solid, such as in the

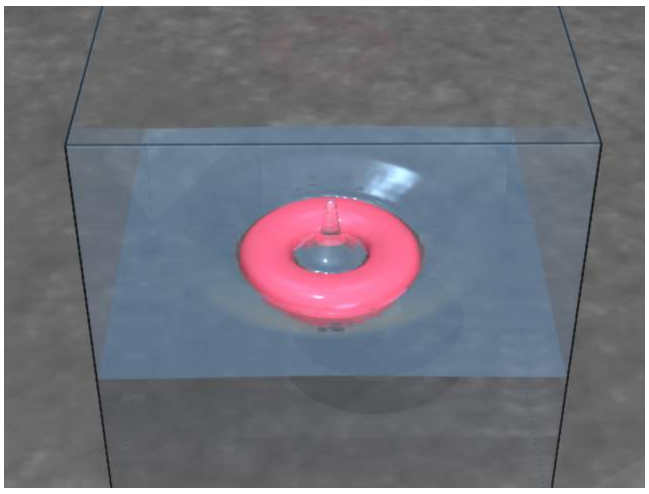

Figure 8: *A soft torus is dropped into a pool of water, showing two-way coupling with a deformable body (100 × 100 × 100 fluid grid, 44k tetrahedra).*

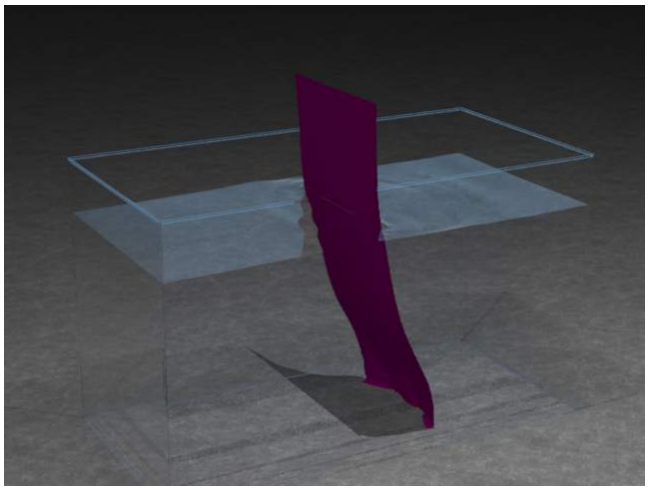

Figure 9: *A sheet of cloth is pulled out of a tank of water (140 × 140 × 70 fluid grid, 2.5k triangles).*

rigid body approach of [Klingner et al. 2006] or [Batty et al. 2007], $D = 0$ and all forces are accounted for in $\mathbf{V}_S^\star$. This is also true for deformable objects if both elastic and damping forces are handled explicitly. In the semi-implicit approach of [Bridson et al. 2003] the elastic forces are handled explicitly but the damping forces are handled implicitly, and D is a symmetric negative definite matrix. Our formulation also allows for a fully implicit approach, as in [Baraff and Witkin 1998], where D is a linearization of both the elastic and damping forces (notably, in the [Baraff and Witkin 1998] approach D is also symmetric, and thus we will assume that it is symmetric throughout the paper). Note when using the fully implicit scheme that D represents the linearization for one Newton-Raphson iteration, and thus repeated solves are required if more iterations are necessary.

5 Momentum Transfer

Whereas the equations for conservation of momentum in Section 4 use $\mathbf{I}$ to represent the momentum transferred between solid and fluid, in general $\mathbf{I}$ is difficult to formulate explicitly, and in particular I_{DC} requires integrating the pressure force on a complex solid/fluid boundary in a mixed dual cell. To conserve momentum, $\mathbf{I}$ should contain all of the I_{DC} terms and the columns of W^T should sum to one so that no momentum is lost. [Guendelman et al. 2005; Losasso et al. 2006a] and the Eulerian grid version of [Chentanez et al. 2006] all interpolate the pressure to the triangle boundary faces of the solid without ensuring that the momentum imparted to the solid is exactly that taken from the fluid. This can lead to both stability problems and inaccurate or nonphysical behavior. The kinetic energy formulation of [Batty et al. 2007] conserves momentum but incorrectly and nonphysically estimates I_{DC} based on the relative volume fractions of fluid and solid within the cell (as discussed in Section 3).

We propose using our back-of-the-envelope procedure in order to avoid explicitly calculating I_{DC}. First, in each mixed dual cell we desire combined equations for the solid and fluid, so instead of using Equation (10) to individually conserve momentum for the fluid portion of the mixed dual cell, we map the fluid mass and momentum to the solid nodes and enforce conservation of momentum there (Equation (11)), which gives

$$\boxed{\tilde{M}_S}\mathbf{V}_S^{n+1} = M_S\mathbf{V}_S^\star + \Delta t D\mathbf{V}_S^{n+1} + W^T\mathbf{I} + \boxed{\Sigma_{DC}\mathbf{W}_{DC}^T(M_F u_F^\star - \Delta t V\nabla_{DC}p - I_{DC})}, \quad (12)$$

where $\tilde{M}_S$ is the nodal mass including both the solid and the lumped fluid and $\nabla_{DC}p$ is the appropriate component of ∇p across dual cell DC. Since $W^T\mathbf{I} = \Sigma_{DC}\mathbf{W}_{DC}^T I_{DC}$, all terms containing I_{DC} drop out. Next we solve conservation of momentum in the solid/fluid system, as explained in Section 6. Afterwards, the velocity of the fluid in the dual cell is interpolated back from the solid using the appropriate rows of W, i.e. $\mathbf{W}_{DC}\mathbf{V}_S^{n+1}$. The rows of W sum to one, and therefore W is an interpolation operator that interpolates the solid velocity to the dual cell faces.

In summary, for mixed dual cells we lump the fluid onto the solid, solve for conservation of momentum in the combined system without needing to form I_{DC}, and then use W to interpolate back the velocity of the fluid. This is similar to our back-of-the-envelope calculation, the final step of which was to construct our pressure profiles given the intermediate pressure $p_{i+1/2}$, which here corresponds to determining I_{DC}. Now that we have u_F^{n+1}, I_{DC} could be calculated, but since our goal was to update the solid and fluid velocities to time t^{n+1}, this is unnecessary.

After fluid lumping and simplification, the solid momentum update equation becomes

$$(\tilde{M}_S - \Delta t D)\mathbf{V}_S^{n+1} + \Delta t W^T V G p = M_S\mathbf{V}_S^\star + W^T M_F\mathbf{u}_F^\star \quad (13)$$

where p is the vector of pressures, G is the standard gradient operator such that Gp gives the gradient of pressure on all dual cells, and V is the volume of a dual cell (which is the same for all dual cells in any of the x, y and z directions). $\tilde{M}_S$ is the diagonal mass matrix created by lumping the fluid mass onto the solid. W^T maps dual cells to solid nodes, so each component of $W^T M_F$ tells us how much to augment the respective diagonal component of M_S. Alternatively, even while solving for conservation of momentum independently on the nodes of the solid and the unmixed cells of the fluid, one could still enforce Equation (10) to be true. This requires mapping Equation (10) itself to the solid nodes using W_{DC}^T and still yields Equation (13), except with $\tilde{M}_S$ equal to $M_S + W^T\bar{M}_F W$, where $\bar{M}_F$ is a diagonal matrix of the masses of the fluid on all mixed dual cells. This gives a symmetric rather than diagonal mass matrix formulation which poses no added difficulty since D is already symmetric and $\tilde{M}_S - \Delta t D$ is the coefficient matrix in the solid equations. We used the diagonal version of $\tilde{M}_S$ in our examples.

We construct W by only considering coupling with surface nodes of the solid, which allows a consistent treatment for thin shells and volumetric objects. Each row of W pertains to a particular dual cell, and we construct it as follows. For each solid node which lies on any triangle face that intersects a given dual cell, we create a weight proportional to the area of the face intersecting that dual cell. Afterwards, these weights are normalized such that each row adds to one.

For each mixed dual cell, we compute the fluid volume by subtracting off the solid volume from the total volume of the dual cell. A more accurate computation of fluid volume (and subsequently mass) could be performed but we found our approximation to be sufficient.

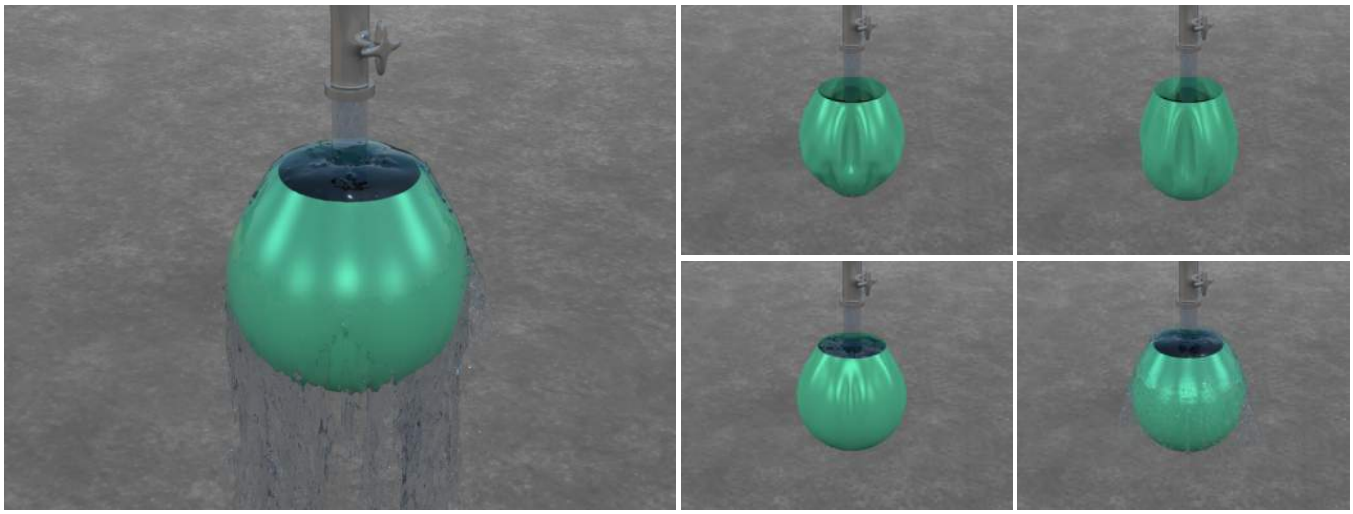

Figure 10: *A stream of water pours into an elastic cloth bag suspended by its rim (100 × 375 × 100 fluid grid, 1k triangles). The bag deforms under the impact of the water and then recovers, filling and expanding until the water overflows and runs down its sides.*

6 Linear System

The system of linear equations for the fluid is typically derived by enforcing incompressibility via

$$\nabla \cdot \mathbf{u}_{SF}^{n+1} = 0 \tag{14}$$

where in our formulation

$$u_{SF}^{n+1} = \begin{cases} u_F^\star - \Delta t G p/\rho & \text{all fluid dual cell} \\ \mathbf{W}_{DC}\mathbf{V}_S^{n+1} & \text{mixed solid/fluid dual cell} \end{cases} \tag{15}$$

This is identical to a voxelized solid formulation, except that WV_S^{n+1} is replaced with the known solid velocity. For convenience, we use a scaled pressure of $\hat{p} = p\Delta t$ and for symmetry we scale Equation (14) by V. Using Equations (13), (14) and (15) we write our linear system as

$$\begin{pmatrix} VG^T \frac{1}{\rho} G & -VG^T W \\ -W^T VG & -\tilde{M}_S + \Delta t D \end{pmatrix} \begin{pmatrix} \hat{p} \\ V_S^{n+1} \end{pmatrix} = \begin{pmatrix} VG^T u_F^\star \\ -M_S V_S^\star - W^T M_F u_F^\star \end{pmatrix} \tag{16}$$

where G is the gradient operator and G^T is minus one times the divergence operator.

6.1 Solving the Linear System

Independently, the solid and fluid systems can be made at least symmetric positive semidefinite, but the coupled system is symmetric indefinite. However, it can still be solved quite efficiently with MINRES (see [Choi 2006]), since it is symmetric. Non-symmetric linear systems are much more difficult to solve [Demmel 1997].

When the mass matrix $\tilde{M}_S$ is diagonal and damping is treated explicitly with $D = 0$, the lower right hand block of our matrix is diagonal and a single Gaussian elimination operation can be used to reduce the two-by-two system by inverting $\tilde{M}_S$ and eliminating V_S^{n+1}. However, this method scales rather poorly. For example, consider a rigid body whose velocity depends on all the pressures that touch its surface. This block Gaussian elimination couples each pressure on the surface to every other pressure on the surface, i.e. each of the $O(n^2)$ pressures (where n is the number of pressure samples in a single dimension) on the surface of the rigid body has $O(n^2)$ nonzero elements in the coefficient matrix for a total of $O(n^4)$ nonzero elements. Although a typical Cartesian fluid mesh has $O(n^3)$ unknowns and a matrix with $O(n^6)$ entries, there are only $O(1)$ nonzero entries per row for a total of $O(n^3)$ nonzero entries. That is, of the potential $O(n^6)$ entries a sparse matrix structure only requires $O(n^3)$, whereas the block reduced form, which is also the form proposed in [Chentanez et al. 2006] and [Batty et al. 2007], requires $O(n^4)$. [Batty et al. 2007] allude to this issue when they state that since they apply a rank 6 update, linear algebra tricks could be applied; however, they do not propose any such techniques. But it seems likely that the application of any such techniques would make the system difficult to precondition. Regardless, when $\tilde{M}_S$ is not diagonal or the damping is not explicit, one cannot perform the block Gaussian elimination.

Indefinite systems are quite common in computational fluid dynamics. For example, consider solving the incompressible Navier-Stokes equations with constant density and an implicit discretization of viscosity,

$$\frac{\mathbf{u}^{n+1} - \mathbf{u}^n}{\Delta t} + \mathbf{u} \cdot \nabla \mathbf{u} + \nabla \tilde{p} = \nu \Delta \mathbf{u}^{n+1} + \mathbf{f} \tag{17}$$

$$\nabla \cdot \mathbf{u}^{n+1} = 0 \tag{18}$$

where $\tilde{p} = p/\rho$. For simplicity we either ignore the $\mathbf{u} \cdot \nabla \mathbf{u}$ term, as is done in Stokes flow, or discretize it explicitly at time t^n and lump it into $\mathbf{f}$. The resulting system of equations looks like

$$\begin{pmatrix} 0 & G^T \\ G & I - \Delta t \nu \Delta \end{pmatrix} \begin{pmatrix} \hat{p} \\ \mathbf{u}^{n+1} \end{pmatrix} = \begin{pmatrix} 0 \\ \hat{\mathbf{f}} \end{pmatrix}. \tag{19}$$

The matrix is symmetric and the lower right hand block is symmetric positive definite, but the nonzero off-diagonal blocks combined with the zero in the upper left block yield an indefinite system. Let $A = I - \Delta t \nu \Delta$. We can perform Gaussian elimination by inverting A to obtain $\mathbf{u}^{n+1} = A^{-1}(-G\hat{p} + \hat{\mathbf{f}})$, which when substituted into the top row gives the positive definite system $G^T A^{-1} G \hat{p} = G^T A^{-1} \hat{\mathbf{f}}$. As mentioned above, we cannot carry out this strategy for our solid/fluid coupling system except when $\tilde{M}_S$ is trivial to invert and the damping is fully explicit, and the same is true here as A^{-1} requires inverting a Laplacian. Computational strategies for solving this classical problem including methods for indefinite systems, MINRES, block Gaussian elimination, inner and

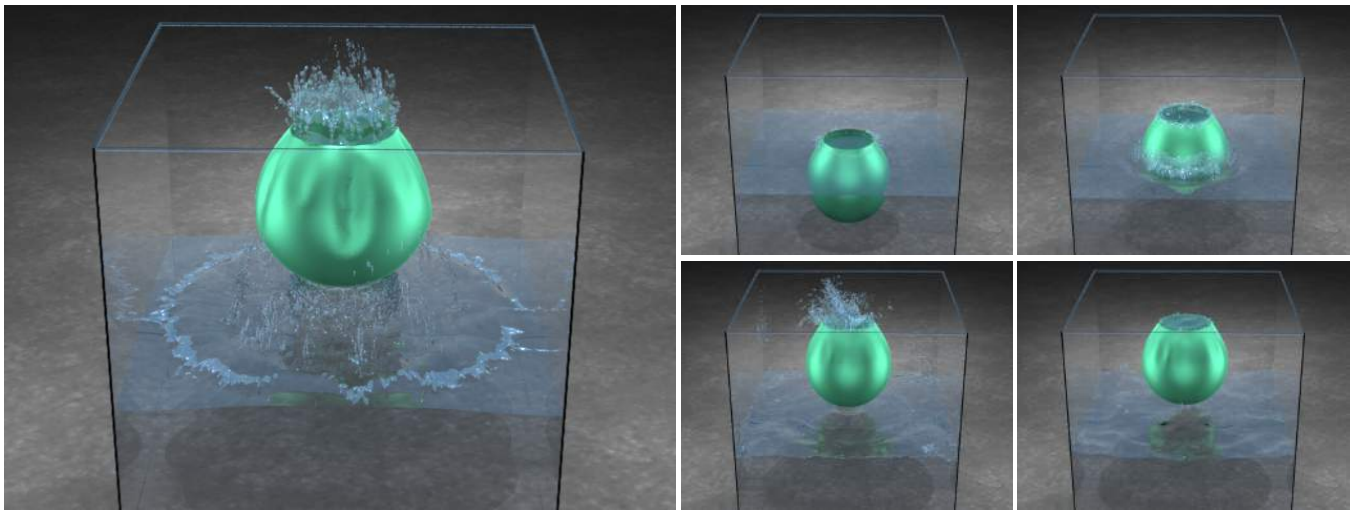

Figure 11: *An elastic cloth bag is submerged in and then quickly pulled from a pool of water, carrying fluid with it (140 × 210 × 140 fluid grid, 1k triangles). The bag bounces as it is raised, expanding and contracting, which causes water to splash out. The bag eventually settles.*

outer iterations where a conjugate gradient method is applied repeatedly to invert A, etc. are quite common, and thus casting our solid/fluid coupling problem into similar form allows us to benefit from previous insights. We consider this a promising avenue for future investigation.

We use an Incomplete Cholesky preconditioner as usual for the pressure rows of our system, and a block diagonal mass-inverse preconditioner for the solid velocity rows. The mass-inverse preconditioner is computed after the fluid mass has been lumped onto the solid nodes.

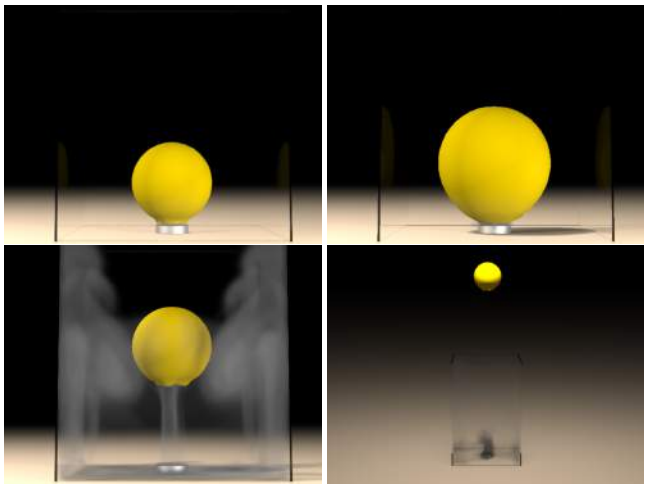

Figure 12: *A balloon is filled by a jet of fast-moving smoke, reaching a state of strong tension (100 × 150 × 100 fluid grid, 1k triangles). The balloon is then released and expels smoke at a very high speed, accelerating upwards, and passes through the edge of the domain without any discontinuities. The high tension and fast velocities highlight the stability of our fully coupled method.*

7 Time Integration

Our two-way coupled time integration scheme hybridizes fluid evolution with a Newmark method for solid integration [Bridson et al. 2003]. Typically Newmark iteration requires one to solve a linear system for the solid velocities twice per time step, and these solves are replaced with Equation (16). The first coupled solve is done with the positions frozen at time t^n and thus all fluid forces are used except convection (i.e. except $\mathbf{u} \cdot \nabla \mathbf{u}$). The second solve is used to update the momentum, and there convection *is* applied. Our method proceeds as follows:

F1: Use all non-pressure based and non-advection based fluid forces (i.e. external forces and viscosity) to advance the fluid velocity to time $t^{n+1/2}$,

$$\mathbf{u}_F^{n+1/2} = \mathbf{u}_F^n + (\Delta t/2)(\mathbf{f} + \nu \Delta \mathbf{u}_F^{n+1/2}). \tag{20}$$

S1: Integrate all explicit solid forces to time $t^{n+1/2}$, $V_S^n \rightarrow V_S^{n+1/2\star}$. Solve Equation (16) for the coupled system to obtain $V_S^{n+1/2}$. The resulting $V_S^{n+1/2}$ is then used to update the solid positions, for collisions, etc, just as in a standard Newmark algorithm (e.g. [Sifakis et al. 2007]). This step follows the standard position update procedures for deformable bodies and rigid bodies, except that the velocity solve incorporates the fluid pressure. After the solve, the fluid pressure and the results of F1 are discarded.

F2: Following [Guendelman et al. 2005], we prevent leaking by forcing the fluid to move with the solid effective velocity, calculated as the change in the position of the solid during S1. A standard fluid Poisson equation is solved using the solid effective velocity mapped onto the Eulerian grid by W as Neumann boundary conditions to project $\mathbf{u}_F^n$. The resulting projected velocity is our leak-proof advection velocity $\mathbf{u}_{ADV}$.

F3: We calculate the intermediate fluid velocity via

$$\frac{(\mathbf{u}_F^\star - \mathbf{u}_F^n)}{\Delta t} + \mathbf{u}_{ADV} \cdot \nabla \mathbf{u}_F^n = \mathbf{f} + \nu \Delta \mathbf{u}_F^\star. \tag{21}$$

Note that the advection velocity $\mathbf{u}_{ADV}$ is used to formulate the rays in the typical semi-Lagrangian scheme [Stam 1999], but the advected quantity is the actual fluid velocity $\mathbf{u}_F^n$. $\mathbf{u}_{ADV}$ is also

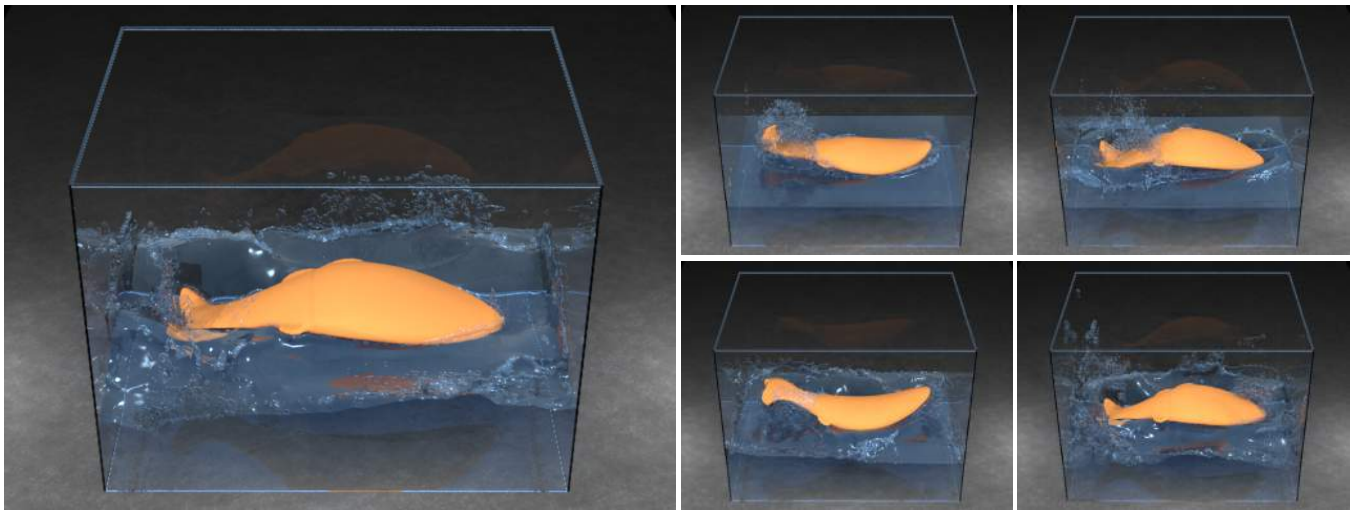

Figure 13: *Water is two-way coupled to a fish with an embedded proportional derivative controlled articulated skeleton and a deformable exterior (192 × 216 × 144 fluid grid, 42k tetrahedra).*

used to advect all other fluid scalar quantities to time t^{n+1}. Since this advection velocity exactly conforms to the effective velocity of the solid, it prevents leaking.

S2: Integrate all explicit solid forces to time t^{n+1}, $V_S^n \rightarrow V_S^\star$. Solve Equation (16) to find V_S^{n+1}, and otherwise carry out the standard algorithms for deformable and rigid bodies (e.g. [Sifakis et al. 2007]). Note that this time the fluid pressure is not discarded.

F4: Using the fluid pressure from S2, project the intermediate fluid velocity $\mathbf{u}_F^\star$ to be divergence free, $\mathbf{u}_F^\star \rightarrow \mathbf{u}_F^{n+1}$.

In summary, there are three implicit solves, two for the coupled system (using MINRES) and one for the fluid (using conjugate gradients). This is the typical situation even in interleaved computations as Newmark time integration requires two conjugate gradient solves and fluids require one. The additional cost here is that the two conjugate gradient solves for the solid have the added coupling to the fluid in the linear system and now require MINRES due to indefiniteness.

8 Rigid Body Implementation

For the sake of exposition, our discussion of the algorithm glossed over some details for the case where the solid is a rigid body, and so we present them here for completeness.

As in the case of a deformable solid, fluid mass is lumped onto the rigid body in a dimension by dimension manner. The modified rigid body mass in dimension i is given by $\overline{M}_i = M_i + \sum_f w_f m_f$, where the sum is over the set of mixed dual cells in dimension i, w_f is the interpolation weight for the rigid body in dual cell f, and m_f is the fluid mass in f. After lumping fluid mass onto the rigid body, we compute its updated center of mass via

$$\overline{M}_i \overline{\mathbf{X}}_i = M\mathbf{X}_i + \sum_f w_f m_f \mathbf{R}_{f,i} \tag{22}$$

where $\mathbf{R}_f$ is the world space position of f. The angular momentum is modified to account for the change in center of mass to obtain

$$\overline{\mathbf{L}} = \mathbf{L} + \mathbf{P}^*(\mathbf{X} - \overline{\mathbf{X}}) \tag{23}$$

where $\mathbf{P}$ is the linear momentum and $\mathbf{P}^*$ represents the cross product matrix. The modified rigid body inertia tensor is

$$\begin{aligned}\overline{I} = I &+ M(\mathbf{X} - \overline{\mathbf{X}})^*(\mathbf{X} - \overline{\mathbf{X}})^{*T} \\ &+ \sum_i \sum_f w_f m_f (\mathbf{R}_f - \overline{\mathbf{X}})^* \mathbf{e}_i \mathbf{e}_i^T (\mathbf{R}_f - \overline{\mathbf{X}})^{*T}\end{aligned} \tag{24}$$

where the first two terms express the inertia tensor of the rigid body in the coordinate system at the new center of mass and the third term accounts for the dimension by dimension lumping of fluid mass onto the body.

Fluid momentum from mixed dual cells is lumped onto the rigid body as well. The momentum from a mixed dual cell f is mapped in the usual fashion for an impulse $\mathbf{j} = m_f u_f^\star \mathbf{e}_i$, i.e. $\Delta\mathbf{P} = \mathbf{j}$, $\Delta\mathbf{L} = (\mathbf{R} - \overline{\mathbf{X}})^*\mathbf{j}$. The total linear and angular momentum mapped is then $\sum_i \sum_f w_f \Delta\mathbf{P}$ and $\sum_i \sum_f w_f \Delta\mathbf{L}$, respectively.

After lumping mass and momentum, we solve Equation (16) to obtain $\overline{\mathbf{V}}$ and ω. Unlumping the fluid mass requires one to modify the rigid body velocity to $\mathbf{V} = \overline{\mathbf{V}} + \omega^*(\mathbf{X} - \overline{\mathbf{X}})$, whereas ω remains unchanged.

9 Examples

We demonstrate coupling of volumetric and thin shell rigid and deformable bodies to both water and smoke. Our examples were simulated in parallel on from four to sixteen processors across a number of four processor Opteron machines and took anywhere from a few minutes per frame to several hours in some extremely high velocity cases. The solid was simulated on a single processor and the fluid was split up across the remaining processors. Figures 3 and 7 demonstrate coupling to rigid bodies with varying density ratios. Figure 8 shows a volumetric deformable object coupled to water. Figures 9, 10 and 11 show cloth coupled to water. Figure 12 shows stability under high tension and high velocities and coupling of cloth to smoke. Figures 7 and 6 show scalability to large numbers of objects. Figure 2 shows interaction between volumetric and thin shell rigid bodies and water. Figure 13 offers an example of the potential for combining our method with other state-of-the-art simulation techniques.

10 Future Work

Our method for time integration requires the solids and fluids to take the same time step and thus for stiff solids it would be beneficial to apply asynchronous or robust and efficient fully implicit methods. This is a promising area for future work. As noted in Section 6.1, solving our symmetric indefinite system is similar to implicitly integrating the well-studied Stokes equations, and thus by casting our equations into similar form we hope to draw on experience from that literature. A promising idea that we have not yet investigated is to map only the normal velocity of the fluid in the dual cell to the Lagrangian solid, while keeping the tangential portion of the velocity on the Eulerian grid to model better slip boundary conditions.

11 Acknowledgments

Research supported in part by a Packard Foundation Fellowship, an Okawa Foundation Research Grant, ONR N0014-06-1-0393, ONR N00014-06-1-0505, ONR N00014-02-1-0720, ONR N00014-05-1-0479 for a computing cluster, NIH U54-GM072970, NSF ACI-0323866, NSF IIS-0326388, NSF ITR-0205671 and NSF CCF-0541148. A.R. was supported in part by a Stanford Graduate Fellowship and J.S. was supported in part by an NSF Graduate Research Fellowship. We would like to thank Bill Dally and Christos Kozyrakis as well as Charbel Farhat for computing resources, Jacob Leverich for helping us use those resources, and Craig Schroeder for the fish model and articulation.

References

BARAFF, D., AND WITKIN, A. 1998. Large steps in cloth simulation. In *Proc. SIGGRAPH 98*, 43–54.

BARGTEIL, A. W., WOJTAN, C., HODGINS, J. K., AND TURK, G. 2007. A finite element method for animating large viscoplastic flow. *ACM Trans. Graph. (SIGGRAPH Proc.) 26*, 3.

BATTY, C., BERTAILS, F., AND BRIDSON, R. 2007. A fast variational framework for accurate solid-fluid coupling. *ACM Trans. Graph. (SIGGRAPH Proc.) 26*, 3, 100.

BRIDSON, R., MARINO, S., AND FEDKIW, R. 2003. Simulation of clothing with folds and wrinkles. In *Proc. of the 2003 ACM SIGGRAPH/Eurographics Symp. on Comput. Anim.*, 28–36.

CARLSON, M., MUCHA, P., VAN HORN, R., AND TURK, G. 2002. Melting and flowing. In *ACM Trans. Graph. (SIGGRAPH Proc.)*, vol. 21, 167–174.

CARLSON, M., MUCHA, P. J., AND TURK, G. 2004. Rigid fluid: Animating the interplay between rigid bodies and fluid. *ACM Trans. Graph. (SIGGRAPH Proc.) 23*, 377–384.

CHENTANEZ, N., GOKTEKIN, T. G., FELDMAN, B., AND O'BRIEN, J. 2006. Simultaneous coupling of fluids and deformable bodies. In *SCA '06: Proceedings of the 2006 ACM SIGGRAPH/Eurographics symposium on Computer animation*, 325–333.

CHOI, S.-C. 2006. *Iterative Methods for Singular Linear Equations and Least-Squares Problems*. PhD thesis, Stanford University.

DEMMEL, J. W. 1997. *Applied numerical linear algebra*. Society for Industrial and Applied Mathematics, Philadelphia, PA, USA.

FAURE, F., ALLARD, J., AND NESME, M. 2007. Eulerian contact for versatile collision processing. Tech. rep., INRIA. http://hal.inria.fr/inria-00149706.

GÉNEVAUX, O., HABIBI, A., AND DISCHLER, J.-M. 2003. Simulating fluid-solid interaction. In *Graph. Interface*, 31–38.

GOKTEKIN, T. G., BARGTEIL, A. W., AND O'BRIEN, J. F. 2004. A method for animating viscoelastic fluids. *ACM Trans. Graph. (SIGGRAPH Proc.) 23*, 463–468.

GUENDELMAN, E., SELLE, A., LOSASSO, F., AND FEDKIW, R. 2005. Coupling water and smoke to thin deformable and rigid shells. *ACM Trans. Graph. (SIGGRAPH Proc.) 24*, 3, 973–981.

HADAP, S., AND MAGNENAT-THALMANN, N. 2001. Modeling dynamic hair as a continuum. *Comput. Graph. Forum 20*, 3.

KEISER, R., ADAMS, B., GASSER, D., BAZZI, P., DUTRÉ, P., AND GROSS, M. 2005. A unified Lagrangian approach to solid-fluid animation. In *Eurographics Symp. on Point-Based Graph.*

KLINGNER, B. M., FELDMAN, B. E., CHENTANEZ, N., AND O'BRIEN, J. F. 2006. Fluid animation with dynamic meshes. In *ACM Trans. Graph. (SIGGRAPH Proc.)*, vol. 25, 820–825.

LOSASSO, F., IRVING, G., GUENDELMAN, E., AND FEDKIW, R. 2006. Melting and burning solids into liquids and gases. *IEEE Trans. on Vis. and Comput. Graph. 12*, 3, 343–352.

LOSASSO, F., SHINAR, T., SELLE, A., AND FEDKIW, R. 2006. Multiple interacting liquids. *ACM Trans. Graph. (SIGGRAPH Proc.) 25*, 3, 812–819.

MÜLLER, M., KEISER, R., NEALEN, A., PAULY, M., GROSS, M., AND ALEXA, M. 2004. Point based animation of elastic, plastic and melting objects. In *Proc. of the 2004 ACM SIGGRAPH/Eurographics Symp. on Comput. Anim.*, 141–151.

MÜLLER, M., SCHIRM, S., TESCHNER, M., HEIDELBERGER, B., AND GROSS, M. 2004. Interaction of fluids with deformable solids. *J. Comput. Anim. and Virt. Worlds 15*, 3–4 (July), 159–171.

RASMUSSEN, N., ENRIGHT, D., NGUYEN, D., MARINO, S., SUMNER, N., GEIGER, W., HOON, S., AND FEDKIW, R. 2004. Directable photorealistic liquids. In *Proc. of the 2004 ACM SIGGRAPH/Eurographics Symp. on Comput. Anim.*, 193–202.

SIFAKIS, E., SHINAR, T., IRVING, G., AND FEDKIW, R. 2007. Hybrid simulation of deformable solids. In *Proc. of ACM SIGGRAPH/Eurographics Symp. on Comput. Anim. (in press)*.

STAM, J. 1999. Stable fluids. In *Proc. of SIGGRAPH 99*, 121–128.

TERZOPOULOS, D., PLATT, J., AND FLEISCHER, K. 1989. Heating and melting deformable models (from goop to glop). In *Graph. Interface*, 219–226.

YNGVE, G., O'BRIEN, J., AND HODGINS, J. 2000. Animating explosions. In *Proc. of ACM SIGGRAPH 2000*, 29–36.

YUKSEL, C., HOUSE, D. H., AND KEYSER, J. 2007. Wave particles. *ACM Trans. Graph. (SIGGRAPH Proc.) 26*, 3, 99.